On the formation of fragments in heavy ion collisions

P.-B. Gossiaux, R.K. Puri, Ch. Hartnack and J. Aichelin*

SUBATECH

Université de Nantes, EMN, IN2P3/CNRS

4, rue Alfred Kastler F-44072 Nantes, France

We investigate in detail the formation of fragments in simulations of symmetric heavy ion reactions between E_{kin} = 50 A MeV and 400 A MeV employing the Q.M.D. model. After a comparison of our results with existing data we investigate with a new algorithm the earliest time point at which the fragments can be identified. It turns out that the fragmentation pattern is determined at the end of the high density phase. Investigating the production mechanism we find at all energies that those nucleons which are finally in a fragment have strong initial - final state correlations in coordinate as well as in momentum space. They are important if one would like to draw conclusions from the mass dependence of dynamical quantities like the flow. The lower the energy the more probable the nucleons traverses the whole reaction partner without suffering a collision. Hence they can preserve their initial correlations and are finally able to form projectile and target like fragments

---

*invited speaker at the INPC 95, Beijing, August 21-26,1995

Why does a nucleus shatter into to several (up to a dozen) intermediate mass fragments (IMF's) if hit by a projectile nucleus? Is this only a statistical process and hence microcanonical phase space models are the proper tool for its description [1] - [2] or is this a dynamical process as conjectured by [3] - [8]?

Despite of extensive efforts of several experimental groups [9] - [14], this question is not finally decided yet. However, the results of the recent and presently most complete experiments by the FOPI collaboration [10] can up to now not be reconciled with the predictions of statistical models. This raises the question of what - if not phase space - is the driving force for multifragmentation. Since the situation of a heavy ion reactions is too complicated to allow an approach starting from first principles the only means at hand for this search are the dynamical models which simulate heavy ion reactions on an event by event basis by following the time evolution of the nucleons. It is all but easy to extract from the complex n body dynamics the underlying physical process. But this is presently the only possibility to identify the physics behind the multifragmentation.

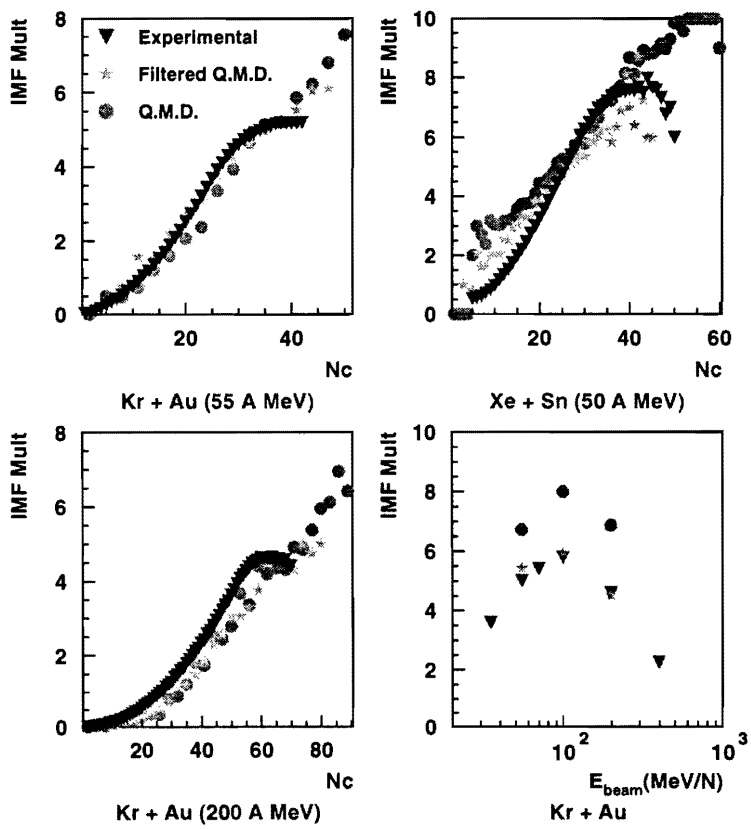

FIG. 1. Multiplicity of IMF's as a function of the number of charged particles. The system Kr + Au has been measured at MSU, the system Xe + Tn represents a result from the INDRA collaboration. The lower right panel shows the average IMF multiplicity as a function of the beam energy

Before any conclusions from the simulation models can be drawn one has to verify that they reproduce the experimental results in a quantitative way. For the Quantum Molecular

Dynamics (Q.M.D.), which will be used in this contribution, this has been done extensively [7,10]. As an example we present here the multiplicity of intermediate mass fragments (IMF's) as a function of the number of charged particles Nc . The system Kr + Au has been measured at MSU [11], the system Xe + Sn has been investigated by the INDRA collaboration [12]. For all systems we present the experimental results, the Q.M.D. results if all particles were detected and the Q.M.D. results filtered by the experimental acceptance filter. We see that the average IMF multiplicity as a function of Nc (and hence as a function of the impact parameter) is well reproduced. This is as well the case for the average number of IMF's as a function of the beam energy as presented in the lower right panel. Here one sees clearly that a beam of 100 A MeV is most suited to investigate the process of multifragmentation.

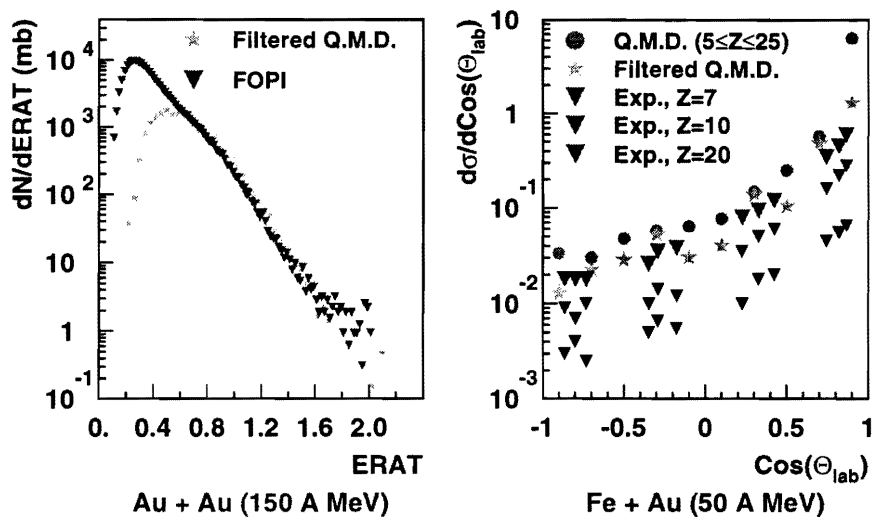

FIG. 2. ERAT-distribution of the system Au+Au at 150 AMeV energy and angular distribution for the system Fe+Au at 50 AMeV.

A more detailed investigation of the reaction at 50 AMeV is available for the asymmetric system Fe + Au where the angular distribution of the fragments have been measured [14]. The comparison with the Q.M.D. calculation is displayed on the right hand side of fig.2. For the Q.M.D. events we have summed over all fragments with charges in between 5 and 25 in order to obtain sufficient statistics whereas the experiment has measured the angular distribution for each fragment charge. We see that the angular distribution of the fragment yield is quite nicely reproduced. Also the absolute value is in reasonable agreement.

On the left hand side of this figure we present the Erat ($= \frac{<p_\perp^2>}{<p_\parallel>}$)distribution (calculated with the Q.M.D. model by the FOPI collaboration) as compared with experiment. The reproduction of the results for central collisions (the calculation stopped at b = 7 fm) demonstrates that the excitation energy of the system is properly described in the Q.M.D. model. The acceptance cuts of the detector lower the Erat value as compared to the unfiltered Q.M.D. events. However, the general statement that Erat = 2, and hence thermal equilibrium, is achieved only in rare events is independent of the acceptance.

This verification of the Q.M.D. model allows to employ this model to proceed further towards a physical understanding of the production process by taking advantage of the fact, that it contains the time evolution of the n-body phase space. The first step towards an understanding of the multifragmentation process is the identification of the time point, at which the fragments are formed. This allows then to investigate the environment in which the formation takes place. This requires a fragment identification already at an early stage of the reaction.

Before one can study the origin of fragments on has to identify the fragments. Up to now the fragments have been identified by a minimum spanning tree (MST) procedure which has also been used to obtain the results displayed in fig.1 and fig.2.

One first simulates the reaction for about 200 fm/c, using Q.M.D.. Then the spatial distance of all nucleons is checked. A nucleon is part of a fragment if there is another one within a distance of r_{min} = 3 fm [6]. This procedure yields stable results, i.e. gives the same fragment pattern for times later than 200 fm/c but cannot be used for earlier times because it only makes sense when the system is very dilute [7].

Recently we have developed a new approach which defines the fragments in phase-space. There nucleons can form a fragment if the total fragment energy/nucl. ζ_i is below a minimum binding energy:

$$\zeta_i = \frac{1}{N^f}\left[\sum_{i=1}^{N^f}\frac{(\vec{p}_i - \vec{p}_{cm})^2}{2m} + \frac{1}{2}\sum_{i\neq j}^{N^f} V_{ij}\right] < E_{Bind}, \tag{1}$$

We take for E_{Bind} = -4.0 MeV if N $\geq$ 3 and E_{Bind} = 0 otherwise. In this equation, N^f is the number of the nucleons in a fragment, $\vec{p}_{cm}$is the center-of-mass momentum of the fragment. This new definition has the advantages that the requirement of a minimum binding energy excludes loosely bound fragments which will decay later. It modifies the definition of Ref. [15], where nucleons can be bound even if the binding energy of the fragment is extremely small. We employ a simulated annealing mechanism to find the most bound configuration and dubbed this approach simulated annealing cluster algorithm (SACA). The result for the reaction Au + Au 400 A MeV, b = 3 fm is presented in fig.3.

The first row shows that the mean density

$$< \rho(t) >= \frac{1}{N}\sum_{i,j=1,i\neq j}^{N}\frac{1}{2\pi L}e^{(x_i(t)-x_j(t))^2/2L} \tag{2}$$

where $2L = 2.16 fm^2$ and the x_i are the centroids of the gaussian wave function of the nucleons. The density reaches its maximum at about 30 fm/c, whereas the collision rate has its peak at about 60-70 fm/c. With increasing time the collision rate becomes negligible whereas the mean density stays constant at about 0.4 ρ_0. This value is an average over all nucleons.It includes the free nucleons which will finally have see a density equal zero as well as the fragment nucleons which feel the density of their fellow nucleons.

The second row shows that SACA finds the heaviest fragment rather early, at a time when the system is still quite dense and interactions among the nucleons are still continuing. This

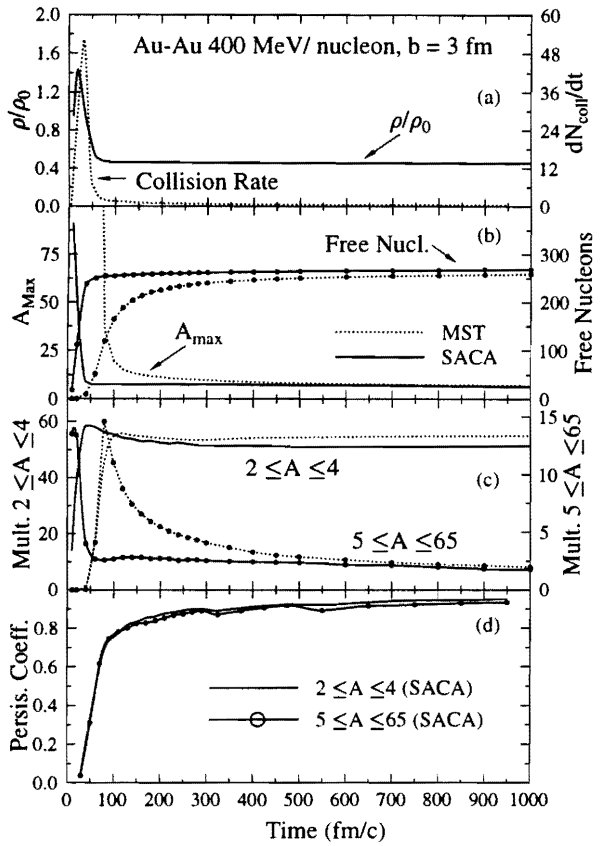

FIG. 3. Evolution of the collision of Au-Au at 400 MeV/nucl. and at an impact parameter b = 3 fm. From top to bottom the rows display the time evolution of the density and of the collision rate, of the size of the heaviest fragments and of the number of emitted nucleons, of the multiplicity of fragments with mass $2 \leq A \leq 4$ and with mass $5 \leq A \leq 65$ and of the persistence coefficient.

gives an indication that the heaviest fragment is formed from the spectator matter which is correct, as we will see later. Note that the MST needs as long as 200 fm/c to find the surviving heaviest fragment. As a consequence SACA predicts also already the asymptotic single particle multiplicity at around 60 fm/c, much earlier than MST. There the heaviest fragment emits continuously loosely bound nucleons until 250 fm/c. These nucleons are still around the heaviest fragment and therefore MST counts them as belonging to the heaviest fragment but are very loosely bound and therefore the most stable configuration is obtained if one consider them no longer as part of the heaviest fragment.

From the third row we see that also the light fragments $2 \leq A \leq 4$ are formed quite early before they are separated visibly in coordinate space. SACA finds the stable pattern at about 50 fm/c, whereas MST identifies them at about 100 fm/c. The formation of intermediate mass fragments ($5 \leq A \leq 65$) is finished after 50 fm/c as well. The MST, however, needs very long (about 300-400 fm/c) until it can identify the final fragments. This is again due to loosely bound fragment nucleons. Their relative velocity with respect to the fragment momentum is small, therefore they rest for a long time in the vicinity of the fragments until they get eventually sufficient energy to escape.

In order to quantify the change of the nucleon content of the fragments between two successive time steps we introduce the persistent coefficient [15,17]. It is one when during a time step the fragment neither looses nor gains a nucleon and 0 when it disintegrates completely. The average persistence coefficient for the fragments $2 \leq A \leq 4$ and $4 \leq A \leq 65$

is displayed in the last row.

One can conclude that the final fragments are formed as early as at 50 fm/c. The persistent coefficient reaches its asymptotic value later due to the (mainly potential) interaction between fragments and between fragments and free nucleons. This interaction changes the details but not the general structure of the fragmentation pattern.

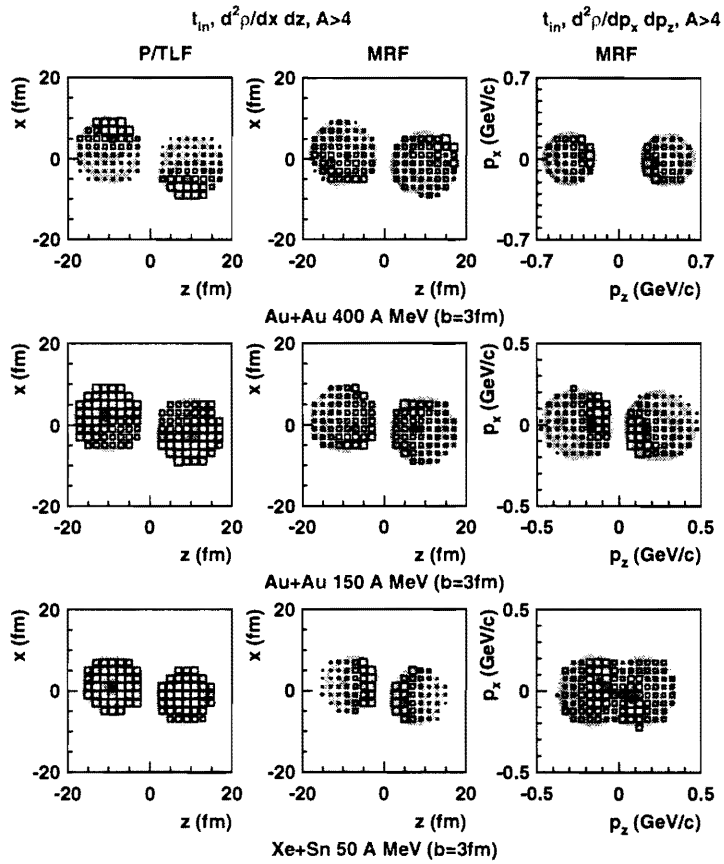

FIG. 4. Initial-final state correlation of nucleons entrained finally in fragments for central collisions and three different reactions. The right column shows the coordinate space correlations of nucleons entrained finally in projectile and target like fragments, the two other columns the coordinate and momentum space correlation of those entrained in midrapidity fragments. The box size marks the probability that a nucleon which was originally (at t=0) at that position is finally entrained in a fragment.

We can conclude that as soon as the violent phase of the reaction is over the fate of the final fragments is already determined. There are first indications from FOPI analyses that the fragment pattern can be formed before the interactions ceases to exits [9]. What is the mechanism which form the fragment at this early time. To investigate this we start with a search of possible initial final state correlations of the nucleons. After having performed a heavy ion collision we trace back the initial phase space point of the nucleons bound finally in fragments and search whether fragment nucleons come predominately from certain regions of phase space. This analysis was done for two classes of fragments, depending on the entrained number of projectile resp. target nucleons at the end of the reaction: Those which

consist predominately (> 75%) of either projectile or target nucleons (projectile/target like fragments PLF/TLF) and those in which we find a mixture of both, called midrapidity fragments (MRF's). In fig. we display some of these correlations.

In each of the 9 panels we display by squares the percentage of nucleons at that initial phase space point which belong finally to P/TLF's or MRF's. The underlying grey values signify the absolute number of nucleons with that fate one finds at this region in coordinate or momentum space. The left column displays the initial final state correlations of PLF's and TLF's in coordinate space for three different central reactions. At the highest energy we observe a verification of the well known participant spectator model. However already at 150 A MeV the structure of the correlation changes. In addition to the correlation in the impact parameter (x) direction we observe as well a correlation in z-direction. This correlation is a consequence of the Pauli blocking of the nucleon nucleon collisions if the final state is already occupied by other nucleons. Whereas initially the nucleons encounter each other with the beam momentum these first collisions lead to a small fireball. Hence the subsequent nucleons scatter with a gas which is at rest in the center of mass system and which has already filled the phase space around midrapidity. Therefore these nucleons have less collisions, i.e. they have a higher change to pass the reaction zone without any collisions, which will lead, as we will understand later, to a larger chance to be finally entrained in a fragment. At the lowest energy the phase space is already quite occupied and even the first interaction taking place between projectile and target nucleons have a high change to be blocked. Therefore most of the coordinate space correlations are gone. However, one has to stress, that the nucleons of projectile like fragments have traversed the whole target nucleus and vice versa. How this happens we will discuss later.

The middle column displays the same correlation for MRF's for the same three systems. As expected at the highest energy these fragments are formed from spectator matter and there is only a small dependence of the correlation on the location of the nucleons in z direction. At 150 MeV/N the situation has changed completely and we observe a strong z but only a weak x dependence of the probability to find the nucleon finally in a fragment. The reason for this we have already discussed. The nucleons at the opposite side of the impact point are not stopped anymore in a way that they mix in momentum space with the nucleons of the reaction partner. Being distinct in phase space means that the probability to form a fragment (which requires a small relative momentum between the nucleons) is small. Hence if those nucleons form fragments they form projectile or target like fragments. This effect is still amplified at the lowest energy we investigated where only nucleons close to the impact point form midrapidity fragments. The others pass this zone without a large dispersion because the Pauli blocking hinders collisions.

The right column finally presents the initial final state correlations of the midrapidity fragments in momentum space. We are not aware that these correlations have been considered as important in the literature. However, we find quite strong correlations. They are extremely important if one wants to discuss the mass dependence of observables like the flow. We observe that the fragment nucleons have already initially a finite transverse

momentum and thus the final transverse momentum has two origins: The flow due to the potential and the momentum already initially present.

For the two reactions with the highest energies we find that the midrapidity fragments are formed from those nucleons which had initially the lowest relative momenta. This is a very strong selection. That means that even the participant matter does not equilibrate completely. Already at the intermediate energy and more strongly at the lowest energy we observe as well a correlation in x direction. This shows that those nucleons form the midrapidity fragments which have already a transverse velocity towards the reaction partner.

As we have seen the fragments can be identified already at the end of the high density stage of the reaction. We have already observed that the fragment nucleons show strong initial final state correlations. There remains the question how the fragment nucleons pass this high density stage in which they are obviously able to conserve their correlations.

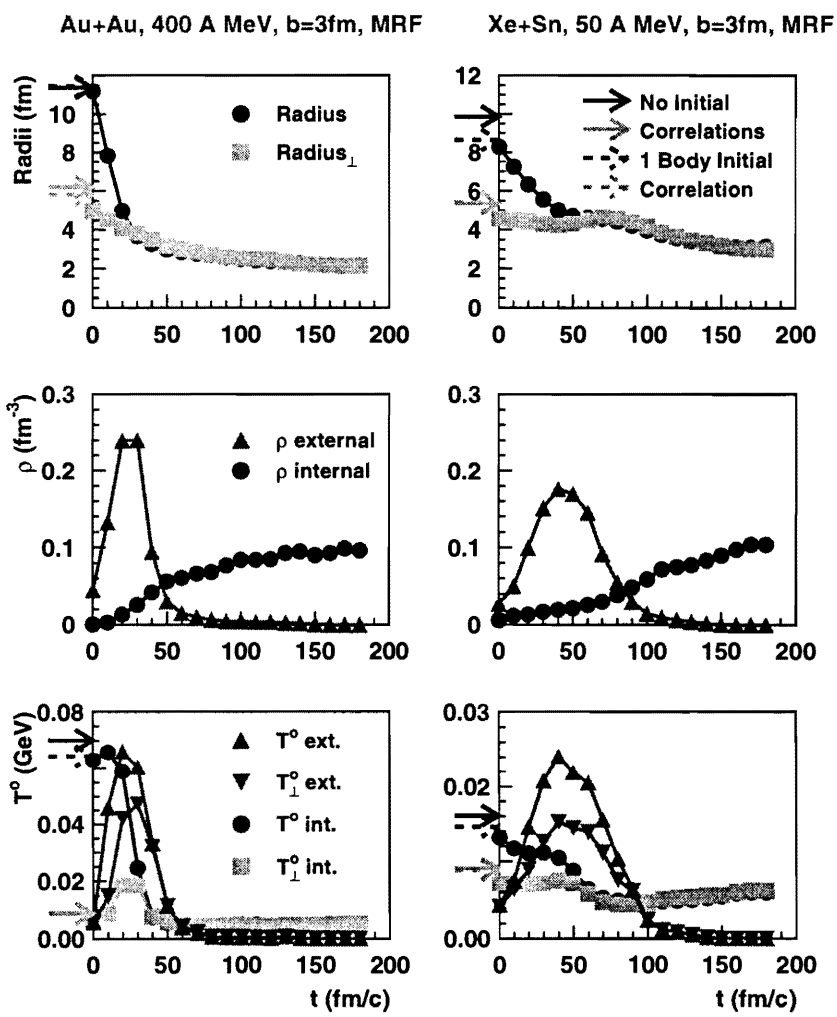

FIG. 5. Time evolution of several quantities averaged over all fragments in comparison with the properties of the environment. For details see text.

This question is addressed in fig. 5. It shows the time evolution of several variables for two reactions, 400 A MeV Au + Au and 50 A MeV Xe + Sn. We have selected central (b= 3fm) collisions and we will concentrate on the midrapidity fragments because they are formed from nucleons which have passed the high density region. In the first line we display the average rms radius of those nucleons which finally form a fragment, as well as their transverse rms radius. In both cases we observe that the transverse radius is initially considerably larger than finally. If one compares the observed value with that expected if one takes randomly the nucleons out of projectile and target (marked by the arrow) one sees that the actual initial value is in between the random and the final value. That means the nucleons are initially not very close together in coordinate space but come together only in the course of the reaction. The second row shows the density around the fragment nucleons. For this purpose we have determined the center of mass of the fragment nucleons and look for the density of particle in a sphere of the radius 3 fm around this center of mass which is caused by nucleons which are finally not part of the fragment. We determine as well the density of the fragment nucleons which contains of course no other information than the rms radius. We observe that the density of the fragment nucleons grows only after the nucleons have passed the high density zone. Before this they do not form a cluster in coordinate space.

The last line finally displays the second moment of the momentum distribution. "Internal" marks the second moment of that distribution for the fragment nucleons. "External" means that of the surrounding nucleons as determined above. We dubbed this quantity sloppily "temperature" although strictly spoken we have no thermal equilibrium. Here we see now clearly the physics. At the moment of high density the nucleons in the surrounding collide and increase their "temperature". This is clearly seen for the transverse "temperature" which is small initially (the above definition yield initially a quite high longitudinal "temperature" due to the beam energy). It increases only little in the course of the reaction. This means that fragment nucleons do not suffer violent collisions which lead to a large momentum transfer. They pass through the reaction zone more or less collectively. They have initially a momentum distribution as if they were chosen randomly among all nucleons but they succeed to escape from the heating up of the system. For the low energy reaction on the right hand side we observe a still more peculiar behaviour. We see that the "temperature" decreases in the course of the time, i.e. the fragment nucleons "cool" in a heated environment. A detailed investigation showed that this is due to scattering of nucleons. Some nucleons which had initially a large relative momentum with respect to the center of mass motion of all fragment nucleons are scattered during the high density phase into a momentum space point which is much closer to the center of mass motion (and therefore these nucleons will be finally part of the cluster). With our definitions this means that scattering decreases the "temperature" of the fragment nucleons. Hence there are not only initial-final state correlations which are conserved and are responsible for fragment formation. In addition correlations are build up in the course of the reaction.

Recently is has been found [18] that the fragment distribution of the ALADIN experi-

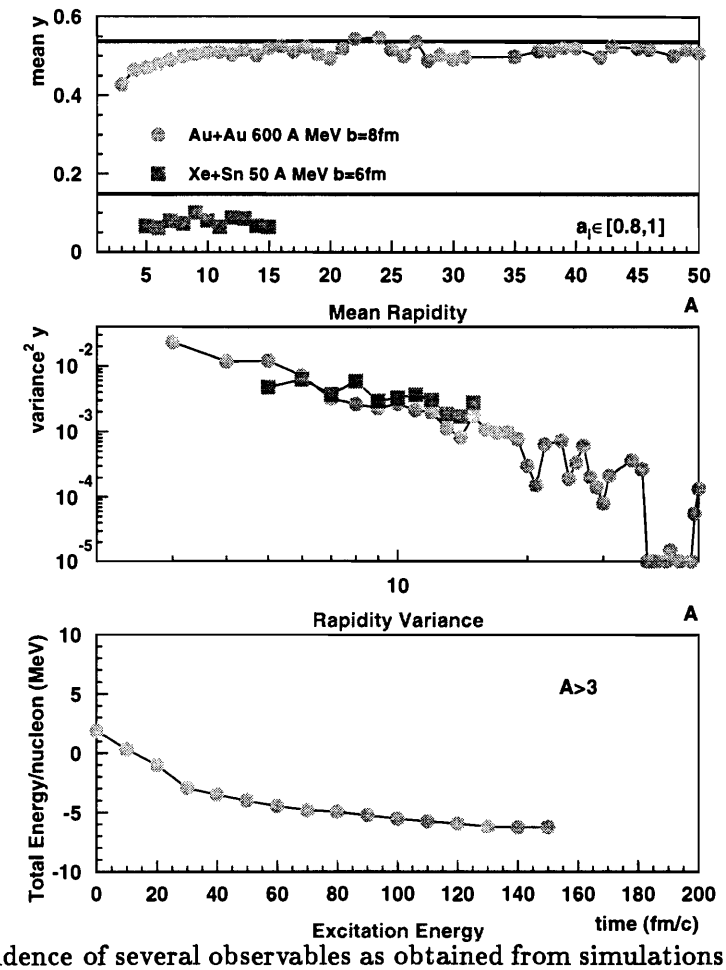

FIG. 6. Mass dependence of several observables as obtained from simulations of the reaction 600 MeV/N Au + Au b=8 fm. We observe a nearly constant average rapidity but a mass dependence of the rapidity width which is much stronger than expected in a thermalized system. The average excitation energy/nucleon in the fragments is quite small and comes to about 1 MeV at the end of our simulation.

ment 600 A MeV Au + Au can be quite nicely reproduced by a statistical model. In this experiments one observes the fragmentation of one of the two nuclei. Most of the fragments come from the projectile spectator matter and have lost very little of their initial momentum. The collaboration conjectured later that this may be an evidence for an equilibration of the system.

To verify this conjecture we made simulations for semiperipheral reactions (b = 8 fm) where one observes a peak in the fragment multiplicity distribution. We find that in the average 192 nucleons entrained in fragments $A > 5$. The smaller fragments as well as nucleons can be less clearer attached to either projectile or target spectator as the intermediate mass fragments. Due to the magnitude of possible exit channels it is not possible in the context of Q.M.D. calculations to investigate in detail whether a distribution expected from a statistical model for a finite particle number is realized. However we can verify whether some necessary but not sufficient conditions for thermalization are fulfilled:

- the average velocity of the fragments has to be independent of the fragment mass, i.e. the fragments may come from a common source
- the variance Δ of the rapidity distribution of the fragments and a possible "temperature" T of the system are connected by

$$\Delta^2 \cdot A \cdot m \;=\; T_{eff}^{dyn}$$

- the excitation energy E in the system is related with the possible "temperature" by the relations

$$T_{eff}^{ex} = \sqrt{\frac{E}{a}}$$

  where a is the level density parameter of about A / (8. MeV^{-1}). and both values of the "temperature" have to be the same.

In fig.6 we investigate these conditions. We see from top to bottom the mean rapidity and the squared variance of the rapidity distribution of the fragments as a function of their mass number, as well as the total energy per nucleon as a function of time.

The mean rapidity of the fragments is slightly below the beam rapidity of 0.54. The heavier fragments approach the beam rapidity whereas the lighter ones are slightly below. Hence the first condition is almost fulfilled.

The squared variance Δ^2 of the rapidity distribution is plotted in a double logarithmic graph. In this graph the second condition results in straight line which is indeed observed for the low mass fragments. The slope of the $variance^2$ is however quite close to -2 and hence quite different from the expected -1 dependence. It is, however, in agreement with data [19], although more precise experiments would be certainly of value. The latest experimental analysis of the Aladin collaboration find a similar dependence of the variance on the fragment mass [21]. The values extracted for T_{eff}^{dyn} are of the order of 15 MeV. This value is compatible with that found experimentally in [20] and agrees also with the preliminary results of the ALADIN collaboration [21]. As mentioned above the mass yield of these results has been successfully described in the framework of a statistical model, however with a much lower "temperature".

This obvious discrepancy in the "temperature" values renders any statement about a possible thermalization premature before a detailed analysis of the momentum distribution of the fragments has been performed.

The energy of the system, i.e. the total energy of those nucleons finally be entrained in projectile (resp.) targetlike fragments with $A > 3$ is displayed in the last row. Initially this energy is high due to some projectile nucleons which become part of the targetlike fragments and vice versa. After the projectile spectator has been disentangled from the fireball and before the spectator matter is disassembled into fragments we observe an excitation energy of about 3 A MeV. At 130 fm/c the system is completely deexcited and the difference between the observed value of - 6.5 A MeV and the value for finite nuclei of - 8 A MeV is partially due

to the relative motion between the fragments. T_{eff}^{ex} is about 4 MeV, in clear disagreement to the value of T_{eff}^{dy} extracted from the spectrum.

At 50 A MeV the situation is completely different. The spectator matter has slowed down to about half of the beam velocity and the variance of the rapidity distribution as well as the mean rapidity is constant.

In conclusion we have demonstrated that QMD is able to reproduce the available data in the energy range of 50 AMeV $\leq E_{lab} \leq$ 400 AMeV to a degree that it most probably contains the proper physics. We have shown that in central collisions the fragments are formed during the high density stage, in some parts due to correlations which are preserved in other parts due to fluctuations caused by collisions. In the high density stage the fragment nucleons are clusters of nucleons with small relative momenta and distances. Hence they present fluctuations in phase space. A different behaviour is found for peripheral collisions. There may be a realm of thermodynamics. However, the use of thermal models may imply that the temperature should be rather regarded as a statistical parameter than as a physical observable. The measurement of energy spectra for fragments $d^2\sigma/dE\,dZ$ will shurly help to answer this question.

---

[1] J.P. Bondorf et al., Nucl. Phys. A **443**, 321 (1985).
D.H.E Gross, Rep. Prog. Phys. **53**, 605 (1990), and references therein.

[2] L.G. Moretto and G.J. Wozniak, Annual Reviews of Nuclear and Particle Science, J.D. Jackson, ed., **43** , 379 (1993).

[3] W. Bauer, G.F. Bertsch and H. Schulz, Phys. Rev. C **69**, 1888 (1992).

[4] W.A. Friedman and W.G. Lynch, Phys. Rev. C **28**, 556 (1983).

[5] J. Aichelin and H. Stöcker, Phys. Lett. B**163**, 59 (1986).

[6] G. Peilert, H. Stöcker, A. Rosenhauer, A. Bohnet, J. Aichelin and W. Greiner, Phys. Rev. **C 39**, 1402 (1989).

[7] J. Aichelin, Phys. Rep. **202**, 233 (1991).

[8] P.B. Gossiaux and J. Aichelin, SUBATECH preprint 95-4, submitted to Phys. Rev. C

[9] M. Petrovici et al., Phys. Rev. Lett. **74**, 5001 (1995).

[10] S.C. Jeong et al., Phys. Rev. Lett. **72**, 3468 (1994)

[11] B. Tsang, Proceedings of the International Workshop XXII on Gross Properties of Nuclei and Nuclear Excitations, Hirschegg, Austria, January 17 -22, 1994 edt by H. Feldmeier and W. Nörenberg

[12] INDRA Collaboration, private communication

[13] M. Begemann-Blaich et al., Phys. Rev.**48**, 610 (1993).

[14] T.C. Sangster, private communication

[15] C. Dorso, and J. Randrup, Phys. Lett. B **301**, 328 (1991).
C. Dorso , and P.E. Balonga, Phys. Rev. C **50**, 991 (1994).
C. Dorso and, J. Aichelin, Phys. Lett. B**345** , 197 (1995).

[16] N. Metropolis, A.W. Rosenblut, M.N. Rosenblut, A.H. Teller, and E. Teller, J. Chem. Phys. **21**, 1087 (1953).
P.J. M. Laarhoven, and E.H. L. Aarts, Simulated Annealing: theory and applications (Reidel, Dordrecht, 1987).

[17] R.K. Puri, Ch. Hartnack and J. Aichelin, to be submitted to Nucl. Phys. A

[18] A. S. Botvina *et al.*, GSI 94-36 (1994).

[19] F.P. Brady et al., Phys. Rev. C50 (1994) R525

[20] J. Dreute et al., Phys. Rev. **C44** (1991) 1057

[21] W. Trautmann et al., private communication